

Available online at www.sciencedirect.com**ScienceDirect**

Procedia Structural Integrity 7 (2017) 214–221

Structural Integrity

Procediawww.elsevier.com/locate/procedia

3rd International Symposium on Fatigue Design and Material Defects, FDMD 2017,
19-22 September 2017, Lecco, Italy

Crack propagation under combined cycle fatigue for a precipitation hardened steel

L. Patriarca^a, S. Foletti^a, S. Beretta^{a,*}, S. Parodi^b, A. Riva^b

^aPolitecnico di Milano, Dept. Mechanical Engineering, Via La Masa 1, Milano 20156, Italy

^bAnsaldo Energia, Via A. Lorenzi, Genova, Italy

Abstract

Compressor blades are generally subjected to Combined Cycle Fatigue (CCF) conditions, where the service cycles are characterized by a low cycle fatigue (LCF) cycle controlled by the centrifugal, pressure and thermal loads superimposed to high frequency loadings at positive load ratios $R > 0.5$ as generated, for example, by the blade vibrations. The recent increasing adoption of renewable energy sources leads to the request to higher level of flexibility for the energy production supplied by gas turbines. The required number of cycles under LCF conditions is increasing leading to lower allowable design stresses. It is thus fundamental to reduce the conservatism adopted with the classical design philosophies. According to a damage tolerance approach, in this activity we have analysed the propagation of small cracks under CCF conditions on a precipitation hardened martensitic steel. The experimental results have mainly shown that the small cracks under CCF are able to propagate at growth rates comparable to the absence of crack closure. This result, together with the Kitagawa diagram, allowed to determine less conservative criteria for the acceptability of surface damages on components subjected to CCF.

Copyright © 2017 The Authors. Published by Elsevier B.V.

Peer-review under responsibility of the Scientific Committee of the 3rd International Symposium on Fatigue Design and Material Defects.

Keywords: combined cycle fatigue; acceptable defects; damage

1. Introduction

Compressor blades can be subjected to Combined Cycle Fatigue (CCF) conditions, where the service cycles are characterized by a low cycle fatigue cycle (LCF) controlled by the centrifugal, pressure and thermal loads, onto which the loadings at load ratio $R > 0.5$ induced by blade vibrations are then superimposed. This peculiar kind of load cycle can be seen as *major load cycles* at $R = 0$, with a target number of repetitions up to 6000 (depending on the type of turbine and the operating profile), and *vibration cycles* at $R > 0.5$. The blade vibrations can take place during startups, baseload and engine shut down operations. A simple engineering assessment can be based only on the LCF

* Corresponding author. Tel.: +39-0223998246 ; fax: +39-0223998202.

E-mail address: stefano.beretta@polimi.it

major cycles or, alternatively, based on the LCF cycles (see Corran and Williams (2007)) plus an infinite life approach for the vibrations. As an alternative, a physically based analysis of the damage would allow to quantify the effect of different cracks/defects onto the prospective life of a compressor blade. This is typically the approach adopted for the vibration cycles, that allowed several authors to analyse the impact of surface degradation and defects onto the prospective safety margins, as discussed by Harkegard (2015) and Schönbauer (2014).

The aim of this research activity, developed under the FLEXTURBINE Project, is to develop a *physically-based* approach for the CCF conditions under basic mechanisms (propagation under LCF [4] + fatigue thresholds). The critical point to be clarified is how the main load cycles at start-ups can affect the subsequent loading cycles at high stress ratios. In detail, if we are prospectively referring to a component subjected to load cycles ΔS at $R > 0$, if the machine is subjected during its life to several missions, then the component will be subjected to pulsating load cycles whose stress range is ΔS_{max} (see Fig. 1.a). The repeated application of those cycles at ΔS_{max} is then able to induce propagation of a defect (or a weak microstructural unit) that otherwise would have remained dormant under the load cycles ΔS . From the point of view of fatigue design, it is then better to refer to a *defect tolerant* design, in which the design stresses are chosen so that inherent material defects are not able to propagate (see Murakami (2002)). The aim of this research is to elucidate how cracks/defects that would be *non propagating* under constant amplitude ΔS , could instead propagate under CCF conditions. The main aim of the present work is thus to achieve a design tool for a robust defect acceptability criteria for a prospective compressor blade subjected to CCF conditions.

Nomenclature

CCF	Combined Cycle Fatigue
COD	Crack opening displacement
CPCA	Compression precracking followed by Constant Amplitude
CPCA	Compression precracking followed by Load Reduction
DIC	Digital Image Correlation
R	Load/Stress ratio
\sqrt{area}	Murakami's parameter for expressing defect size
ΔS_{max}	Stress range for the pulsating load cycle corresponding to turbine startup
ΔS	Stable stress range during service
$\Delta\sigma_w$	Fatigue limit for a given defect size
$\Delta\sigma_{wo}$	Fatigue limit for a smooth specimen (no defect)

2. Material and experiments

2.1. Fatigue tests

The material characterized is a martensitic precipitation hardening steel. The cylindrical specimens were cut into two different geometries as shown in Fig. 2.a and 2.b. The smooth cylindrical specimens were used to test the material for determining the S-N diagram and fatigue limit at $R=0$ and the fatigue limit at $R = 0.5$. Tests were carried out on a 100 kN RUMUL resonant testing machine. The second specimen geometry was adopted to introduce a small artificial defect in one of the two flat surfaces to study the effect of a crack in the endurance limit at the two load ratios. Under the conservative assumption of the presence of surface defects (scratches, pits) on the compressor blades, it was decided to introduce an EDM micronotche with a size $\sqrt{area} = 190\mu m$, a dimension bigger than the largest martensitic grains of the microstructure. Since the fatigue tests on the micronotched specimens of precipitation hardened steels are in general characterized by very short or negligible cracks (see Murakami (2002)), the specimens were subjected to compression-precracking for 10^7 cycles obtaining cracks of the order of 20-40 μm at the the edge of the micronotches (see Fig. 1.b). According to the concepts by Murakami (2002), these defects can be treated as small cracks.

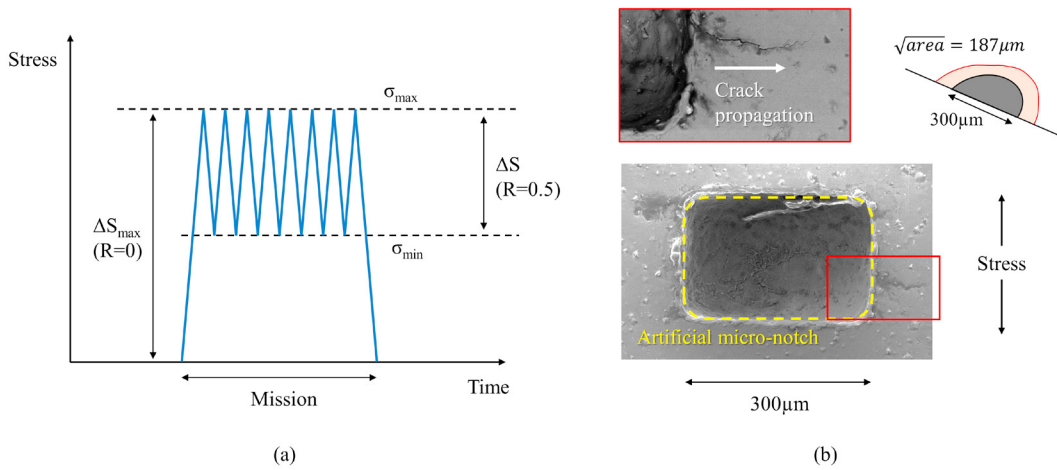


Fig. 1. Schematics of the problem addressed in this research: a) CCF is characterized by a major load cycles and the blade vibrations at load ratio $R = 0.5$; b) the prospective propagation of short cracks under $\Delta S_{max} + \Delta S$.

The results showed that the fatigue limit of smooth specimens is in good agreement with the Goodman diagram suggested by FKM Guideline (2012) (see Fig. 2.c). The fatigue limit in presence of the microcracks shows a large decrease. This reduction provides a qualitatively indication on the value of the safety margins needed in the design.

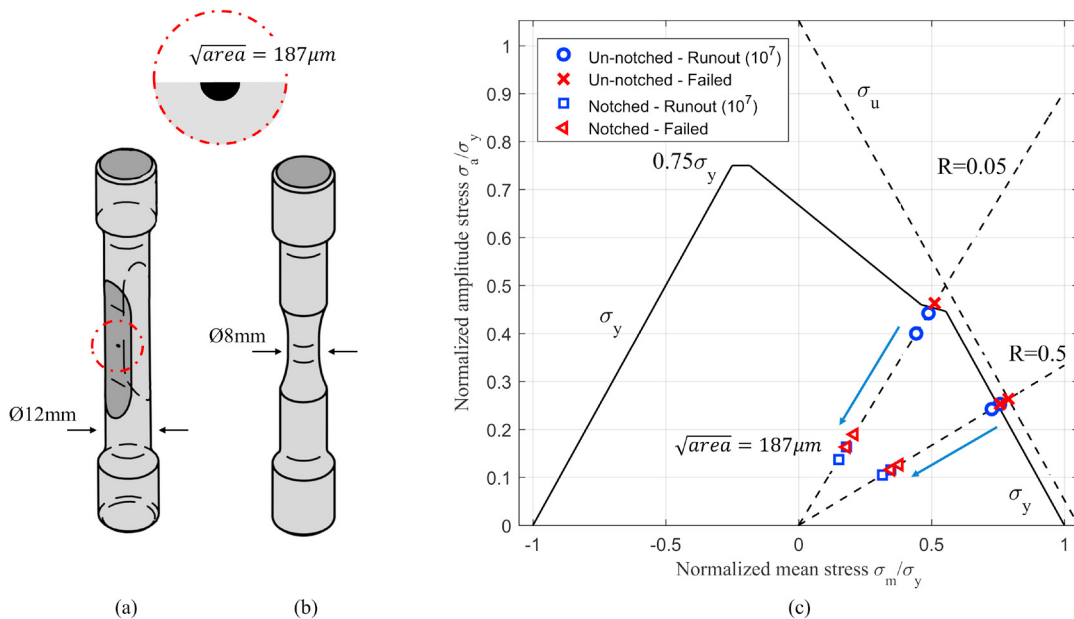


Fig. 2. Fatigue tests under constant amplitude loading: a) micro-notched specimens; b) smooth specimens; c) the resulting Haigh diagram.

2.2. Crack propagation and threshold experiments

A series of tests were carried out on *three point bending* tests in order to determine the crack growth rate data of the material. The tests were carried out according to the CPLR technique (see Carboni et al. (2011)): after compression

pre-cracking, the crack growth is stabilized at a suitable ΔK so that the crack growth rate reaches the range $1 - 2 \cdot 10^{-9}m/cycle$. Then the specimen is subjected to a ΔK -decreasing with conventional load shedding. Test results have been interpolated with the NASGRO propagation equation (see NASA (2006)). Long crack growth threshold results are shown in Fig. 3.a together with interpolation with the NASGRO model. The Kitagawa-Takahashi digram (Fig. 3.b) was then derived by using the long crack thresholds and the endurance limits at $R = 0.05$ and $R = 0.5$ with a modified El-Haddad model (as proposed by Beretta et al. (2005)):

$$\Delta\sigma_w = \Delta\sigma_{wo} \cdot \sqrt{\frac{\sqrt{area_o}}{\sqrt{area} + \sqrt{area_o}}} \tag{1}$$

where $\sqrt{area_o}$ is the El-Haddad parameter is expressed in terms of \sqrt{area} . The resulting $\sqrt{area_o}$ is approx. $20\mu m$, which makes the short cracks constituted by EDM micronotches + pre-cracks almost equivalent to a long crack for the examined steel (usually a crack is long when $a > 10a_o$ see Suresh (1998)). A threshold test at $R = 0.05$ was carried

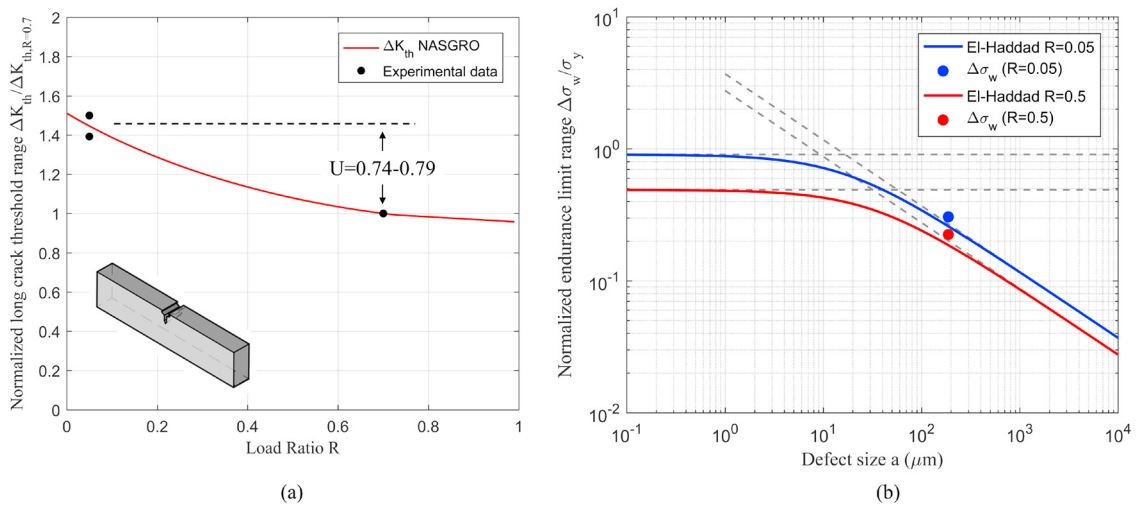


Fig. 3. Threshold experiments: a) ΔK_{th} on long cracks; b) the Kitagawa-Takahashi diagrams at $R = 0.05$ and $R = 0.5$.

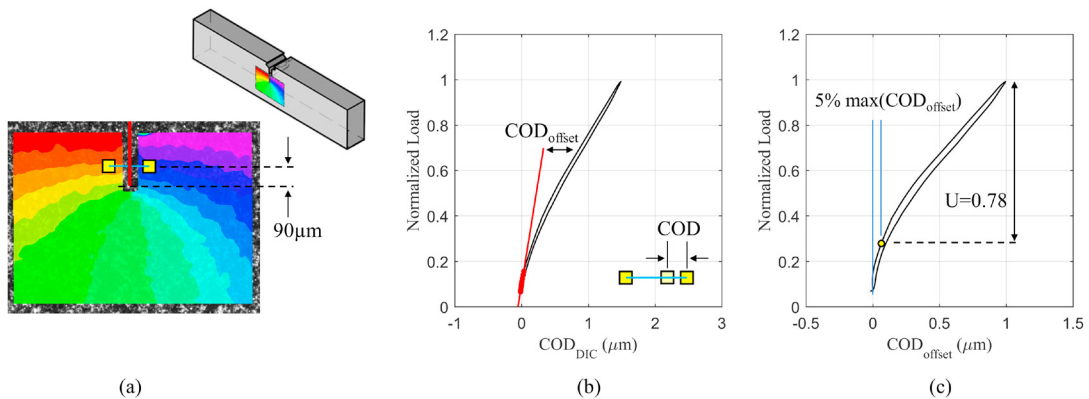


Fig. 4. Closure measurements during CPCA tests: (a) virtual extensometer behind the crack tip; (b) $Normalizedload - COD_{DIC}$ cycle; (c) $Normalizedload - COD_{offset}$ and determination of closure load.

out under CPCA and, at the stress level at which the crack starts to propagate, the closure levels were measured by

DIC during the load cycles by using the virtual extensometer technique. The virtual extensometers were positioned at a distance of 80 – 100 μm behind the crack tip. The load vs. crack opening displacement cycles (i.e $P - COD$ cycles) cycles have been analyzed for estimating the closure level. In details, we calculated $COD_{offset} = COD_{meas} - COD_{linear}$, where the linearized COD_{linear} was estimated from the first part of the $P - COD_{DIC}$ cycle (Fig. 4.b). The $COD_{offset} - P$ cycle was successively used to determine the opening load according a deviation of $0.05 \cdot COD_{offset,max}$ from zero of the COD_{offset} signal. As shown in Fig. 4.c, the measurements have returned a mean value:

$$U = \frac{\Delta K_{eff}}{\Delta K} = 0.78 \quad (2)$$

Considering that at any R , $\Delta K_{th} = \Delta K_{th,eff}/U$, it can be seen from Fig. 3.a that this value is consistent with the long crack growth threshold experiments.

2.3. CCF tests

The micronotched specimens survived to constant amplitude fatigue tests were then subjected to CCF tests. The crack growth rates measured during these CCF tests were then compared with the crack growth rate curves obtained for long crack tests. The stress range ΔS for the block cycles at load ratio $R = 0.5$ corresponds to the endurance limit $\Delta\sigma_w$ as shown in the Kitagawa diagram (Fig. 3.b). Once this stress range ΔS ($R = 0.5$) is fixed, the stress range for the cycles at load ratio $R=0$ is determined according $\Delta S_{max} = 2 \cdot \Delta\sigma_{w,R=0.5}$. As it can be noticed from Fig. 3.b, the fatigue limit at $R=0$ in presence of the microdefects results to be $\Delta\sigma_{w,R=0} < 2 \cdot \Delta\sigma_{w,R=0.5}$, so the pulsating load cycles ΔS_{max} are able to induce crack propagation. Based on this stress definition, three types of experiments were conducted and compared: (i) Crack propagation under pulsating $R=0$ cycles (Fig. 5.a); (ii) CCF with ratio 1 : 100 cycles (Fig. 5.b); CCF with ratio 1 : 10000 cycles (Fig. 5.c). The crack growth curves for these testes are shown in Fig. 5.d where the number of cycles refers to the number of pulsating cycles at $R=0$. In terms of crack growth rates, Fig. 5.e shows that during the CCF tests, the growth rate of the short cracks is accordance with the crack growth rate at $R=0.7$.

3. Discussion of results and application

The results of the threshold experiments clearly show that the propagation of short cracks starting from a defect size of the order of 200 μm can be considered as a long crack propagation, in fact the El-Haddad parameter $\sqrt{area_o}$ is approx. 20 μm . The same result is also shown by the CPCA tests, where the closure measurements have shown a stabilization of the closure (or alternatively a stabilization of the ΔK_{th} value during the CPCA tests) with a crack advance less than 200 μm .

From this point of view, it could be expected that the propagation of short cracks from the EDM notches could be described with a simple *propagation model* based on the NASGRO propagation equation and a simple *no interaction* between the stress levels. The adoption of this concept leads to estimates that are quite close to the experimental results, as it can be seen from the crack growth predictions versus the experimental data reported in Fig. 6.

3.1. Prospective defect tolerance under CCF

The good agreement between experiments and predictions allowed to exploit the propagation model for exploring the effect of CCF cycles upon the maximum allowable stress range for a compressor blade. Considering a simplified scheme of 18000 missions of 6 hours (that could correspond to a very long service of 30 years with 2 cycles per day), in which the stress ratio is $R = 0.5$ and the frequency for the stress oscillations is 100 Hz, we have explored two different design scenarios (under the condition $S_{max} = 2 \cdot \Delta S$):

- # 1) all the δS_{max} cycles are considered first and then the ΔS cycles are subsequently applied (see Fig. 7.a);
- # 2) the CCF sequence of a ΔS_{max} cycle every $2 \cdot 10^6$ cycles ΔS cycles at $R = 0.5$.

The long service of the compressor blade implies a number of cycles greater than 10^8 cycles and so *very high cycle fatigue* - VHCF - could be a concern. This phenomenon has been taken into account considering the results by Sander et al. (2014), who showed a stable propagation in VHCF at ΔK levels below ΔK_{th} with a characteristic slope of the $da/dN - \Delta K$ diagram. The analysis has been carried out finding (by trial and error) the maximum ΔS that could

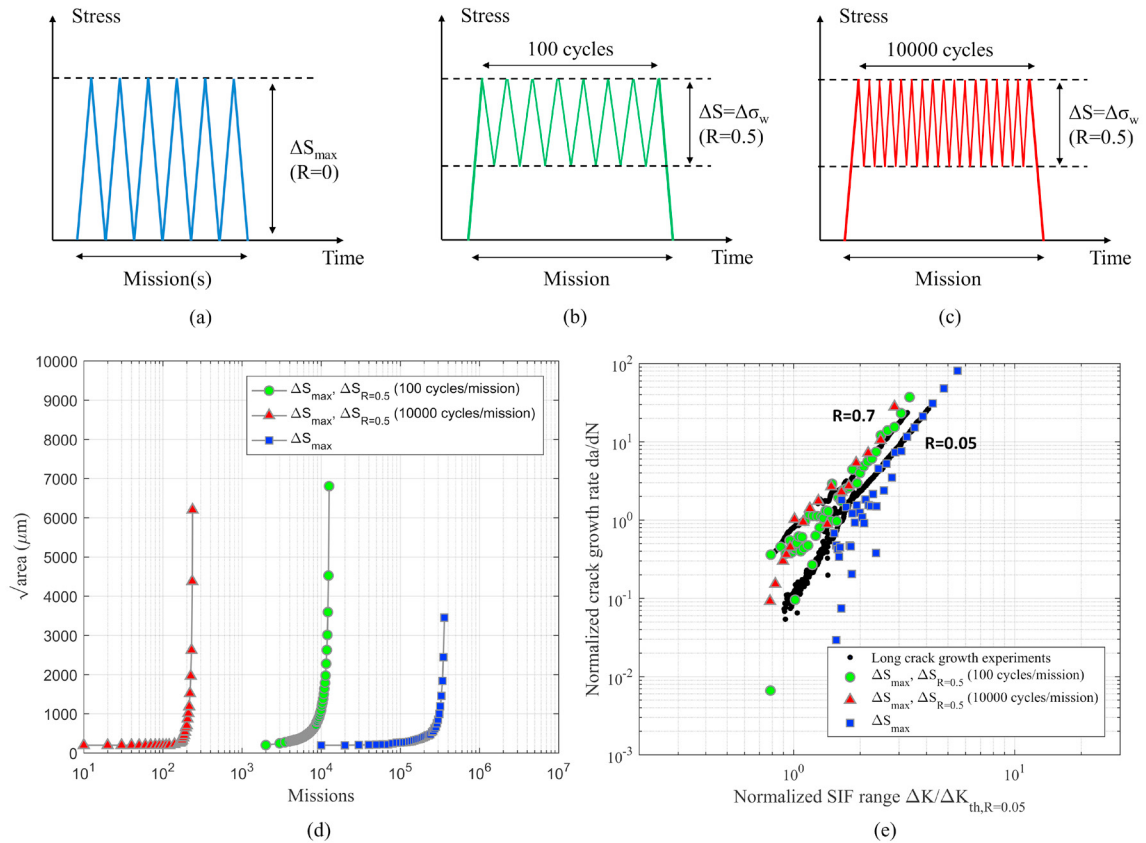


Fig. 5. CCF tests on specimens with micronotches: a-b-c) the three load cycles scenario investigated; d) the crack growth curves in terms of cycles at $R=0$ (number of missions); e) the $da/dN - \Delta K$ data compared with the long crack growth rates at constant amplitude.

ensure a stable propagation $\Delta a < 100 \mu m$ during a prospective service of 30 years. The summary of the results are schematically shown in Fig. 7.b. In particular, the design scenarios are compared in terms of the allowable maximum ΔS compatible with the presence of a defect of $190 \mu m$. The CCF scenarios #1 and #2 show a significantly lower permissible ΔS in comparison with the constant amplitude (CA) loading which does not consider the effect of the high frequency $R = 0.5$ cycles. Accordingly, the CA is found to be the most un-conservative prediction. Meanwhile, it is worth remarking that scenario #1 represents a conservative assumption for component design.

3.2. Future developments

The next steps of the research, to be done within the EU project FLEXTURBINE will be:

- The improvement of the crack propagation simulation which considers the variation of the opening stress with crack advancement $S_{op} - \Delta a$ determined by the CPCA tests according the R-curve concepts by Zerbst et al. (2016);
- A probabilistic analysis for a prospective very low failure probability, in order to obtain maps $\Delta S - \sqrt{area}$ to support FOD assessment and life extension of the compressor blades.

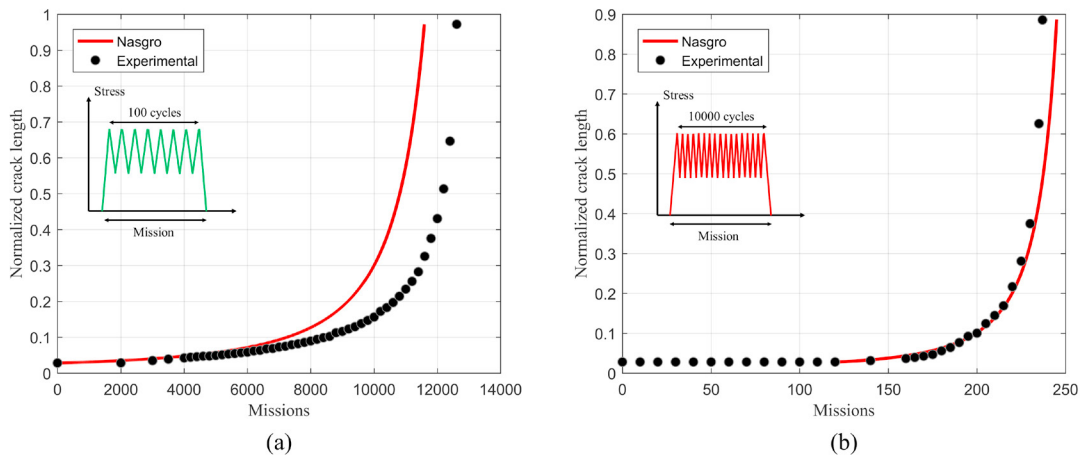


Fig. 6. Analysis of the CCF tests with a *no interaction model* based on NASGRO propagation equation: a) test with blocks of 100 cycles at $R = 0.5$; b) test with blocks of 10000 cycles at $R = 0.5$.

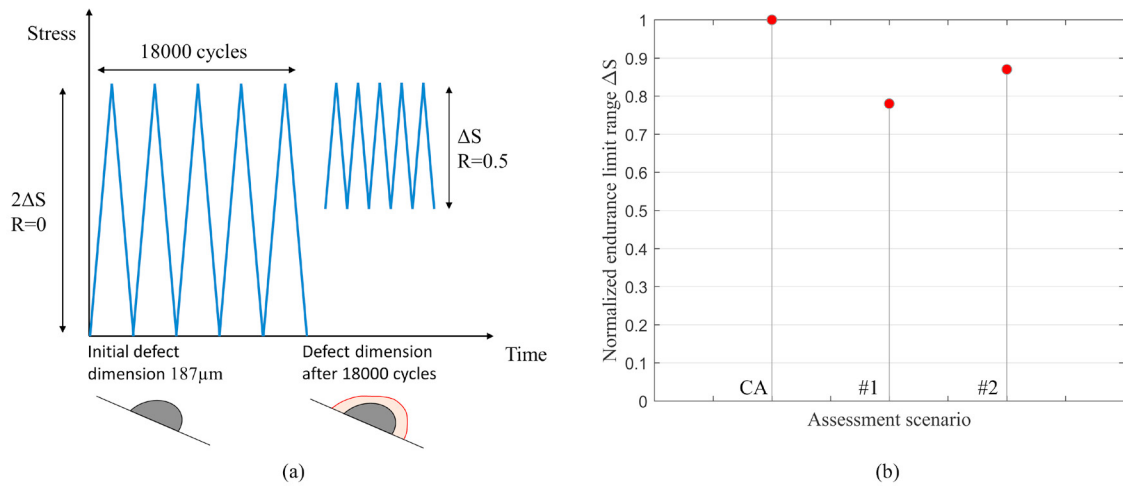


Fig. 7. Fatigue assessment for CCF: a) the conservative scenario #1; b) the resulting maximum ΔS that can be applied for a defect with $\sqrt{area} = 190 \mu m$ under the different scenarios.

Acknowledgements

The research was carried out within the EU Project FLEXTURBINE (Grant n. 653941). The authors acknowledge permission by the Flexurbine Consortium to publish the present paper.

References

Beretta, S., Ghidini, A., Lombardo, F., 2005. Fracture mechanics and scale effects in the fatigue of railway axles. *Engineering fracture mechanics* 72, 195–208.
 Carboni, M., Patriarca, L., Regazzi, D., 2011. Determination of δk_{th} by compression pre-cracking in a structural steel, in: *Fatigue and Fracture Mechanics: 37th Volume*. ASTM International.
 Corran, R., Williams, S., 2007. Lifting methods and safety criteria in aero gas turbines. *Engineering Failure Analysis* 14, 518–528.
 FKM Guideline, 2012. *Analytical strength assessment of components in mechanical engineering*. 6th, rev. ed., VDMA-Verl.

- Harkegard, G., 2015. Shortcrack modelling of the effect of corrosion pits on the fatigue limit of 12% Cr steel. *Fatigue Fracture Engng. Mater. Struct.* 38, 1009–1016.
- Murakami, Y., 2002. *Metal Fatigue: Effects of Small Defects and Nonmetallic Inclusions*. Elsevier, Oxford.
- NASA, 2006. *Fatigue crack growth computer program NASGRO version 4.2-Reference manual*. NASA Johnson Space Center.
- Sander, M., Müller, T., Lebahn, J., 2014. Influence of mean stress and variable amplitude loading on the fatigue behaviour of a high-strength steel in vhc regime. *International Journal of Fatigue* 62, 10–20.
- Schönbauer, B., 2014. Fatigue life estimation of pitted 12% Cr steam turbine blade steel in different environments and at different stress ratios. *Int. J. Fatigue* 65, 33–43.
- Suresh, S., 1998. *Fatigue of materials*. Cambridge university press.
- Zerbst, U., Vormwald, M., Pippan, R., Gaenser, H.P., Sarrazin-Baudoux, C., Madia, M., 2016. About the fatigue crack propagation threshold of metals as a design criterion—a review. *Engineering Fracture Mechanics* 153, 190–243.